International Journal of Electrical, Electronics and Data Communication, ISSN(p): 2320-2084, ISSN(e): 2321-2950
Volume-8, Issue-6, Jun.-2020, http://iraj.in

DESIGN, DEVELOPMENT AND ANALYSIS OF BLADELESS THRUSTER

[1]ANUTHA M A, [2]APARNA RAVI, [3]ARUN LUKE DSOUZA, [4]SUNIL KUMAR, [5]TEJASWINI G

[1]Assistant Professor , Department of Aeronautical Engineering, Dayananda Sagar College of Engineering, ShavigeMalleshwara Hills, Kumaraswamy Layout, Bangalore -78, India
[2,3,4,5]Student, Department of Aeronautical Engineering, Dayananda Sagar College of Engineering, ShavigeMalleshwara Hills, Kumaraswamy Layout, Bangalore -78, India
E-mail: [1]anumade91@gmail.com, [2]aparnar97@gmail.com, [3]arunluk77@live.com, [4]sunilsemailid@gmail.com, [5]tejaswinigovindaraju98@gmail.com

Abstract - Conventional multi-copters include a plurality of propellers designed to provide lift, propulsion and altitude control of the UAV. Inspired by the Dyson bladeless fan, the proposed thruster has the significant advantage of a bladeless technology in terms of safety. The thruster is composed of a vertical inlet duct with an Electric Ducted Fan and a special nozzle ring. The pressure difference created through the airfoil-like cross- section of the ring combined with the Coanda effect helps to create at a thruster that has no externally rotating blades or propellers.

Keywords - Bladeless Thruster, Coanda Effect, Entrained Air, Induced Air

I. INTRODUCTION

The idea of a Bladeless Thruster system was inspired by the British tech manufacturer Dyson when they released merchandise called the Air Multiplier – a quieter fan, more power-efficient, safer and most importantly 'bladeless'. The mechanism of the thrusters employed will be composed of two parts – an Electric Ducted Fan (EDF) or a specifically designed compressor and a discharge frame.
The purpose of the electronic components is to provide a form of suction of air from the surroundings and channel it towards the discharge frame. The discharge frame is held in position to accelerate the incoming flow. Similar concepts of pressure differences over the surface of the airfoil are employed across the nozzle ring. The induced airflow through the suction mechanism creates a region of low pressure over one end of the ring. The combination of the induced flow and the accelerated flow creates a high-pressure area across the other end of the ring. The fundamentals used here are basic concepts of lift generation and thus it can be employed in creating a propulsion system that creates a state-of-the-art bladeless design on an Unmanned Aerial Vehicle (UAV).

II. EXPERIMENTAL DETAILS

2.1. Feasibility of Bladeless Thruster

Referring to various research papers, the ideology of a bladeless propulsion system was conceived through Dyson's bladeless fan. Based on the research by Daniel Valdenegro et al [1] the thruster assembly is composed of two parts -an EDF or a compressor and a discharge frame with an inlet.The EDF will provide high velocity or high-pressure air to the discharge frame, which in turn creates a suction of air termed as induction through the discharge frame. The surrounding air is drawn into the injected flow and is termed as entrainment. Here, fundamental concepts of lift are involved that creates a low-pressure on the suction surface of the airfoil and a high-pressure on the pressure surface of the airfoil.
The induced airflow creates a low-pressure area on the periphery of the ring. The combination of induced airflow and injected airflow create a high- pressure area in the component. the fundamental concept of low- and high- pressure areas for creating lift are employed. This concept of a propulsive system can be applied to create the first start of the art bladeless UAV . A change in pressure from the inlet and outlet is necessary to create thrust from a propulsion system. A net change of pressure in the flow causes an additional change in momentum.

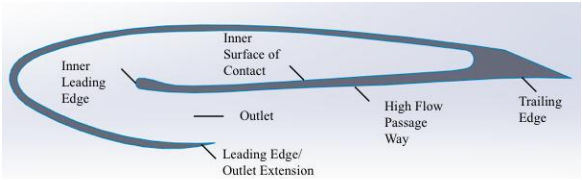

Fig.1. Airfoil Parts.

2.2. Thruster Cross-Section

In order to achieve a better performance, an airfoil profileFig.1 was selected among standardized airfoils and evaluated as the thruster's cross-section, because it has a high curvature (good Coanda surface). Thus, an enhanced suction of air from the rear portion of the discharge ring can be achieved. The airfoil like cross-section of the nozzle is essential to increase the performance of the thruster. The airfoil can be modified to obtain maximum thrust by varying parameters like throat size, inlet duct length, hydraulic diameter and taper angle. The capacity to acquire greatest thrust from each thruster necessitates a uniform flow (laminar) of air that is not constrained

by any horizontal flow components along its thrust axis (turbulence).

Another important concept that needs to be understood completely in order to successfully design the thruster is the Coanda effect and subsequently the Coanda ejector.

The Coanda ejectorFig.2 is an axisymmetric device that uses the injected primary flow on the inward curved surface of the geometry while entraining a secondary flow on the outer curved surface. A Coanda ejector is primarily used to deliver a high ratio of the induced mass flow rate to the injected mass flow rate. The ratio of induced mass flow rate to injected mass flow rate is called w factor.

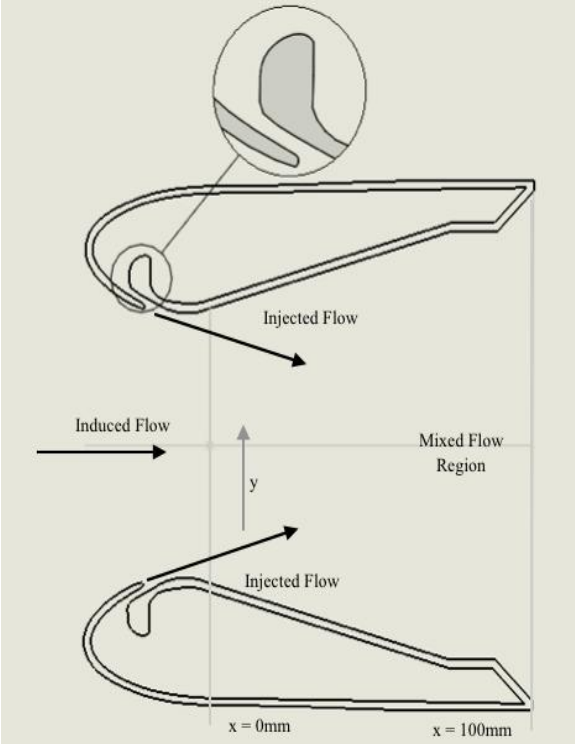

Fig.2. Coanda Ejector Surface. Airfoil Parts.

The primary flow is provided by a compressor, which follows the curved contour of the ejector after flowing through the throat, due to Coanda effect. A turbulent mixing zone is developed as a result of expansion/compression waves created due to the pressure at the outlet section.

The effects of pressure ratio, outlet and ejector configurations on the system performance are estimated based on the performance parameters. The mixing layer growth is crucial to enhance the performance of the Coanda ejector as it controls the w factor and the mixing length. Based on the velocity profile shape Fig.2, which is measured by the amount of the outlet throat gap, the mixing characteristics can be approximated. Complete mixing ratio between the primary and the secondary or induced jets is indicated by the flattened shape of the profile. To yield a better ejector performance, these characteristics need to be achieved in a section closer to the inlet.

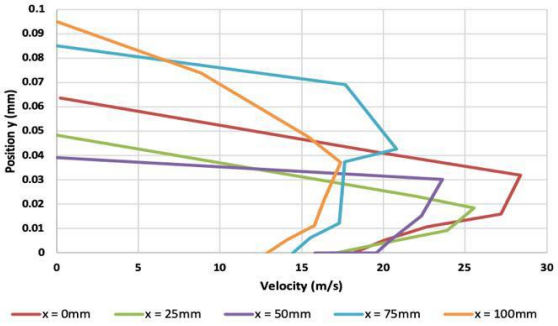

Fig.3. Velocity magnitude in five sections of the thruster.

2.3. Design of Thruster Cross- Section

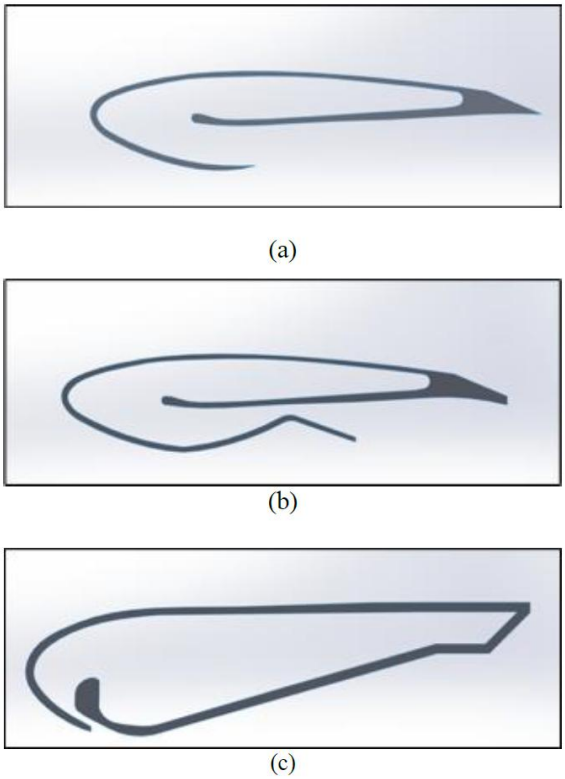

Fig.4. (a) Design 1 (b) Design 2 (c) Design 3.

The airfoil cross-section of the thruster has evolved primarily from Dyson's bladeless fan's cross- section. The best thruster design was chosen after running a CFD 3D Analysis of the thruster.The cross-section design and analysis were done using SolidWorks. A k-epsilon model was preferred as the required turbulence model. SolidWorks 3D CAD data is directly used for fluid flow simulation using SolidWorks Flow Simulation using built-in functions. The fluid domain is automatically generated based on the geometry and is then revised for any design changes. Flow conditions are well-defined directly on the SolidWorks CAD model.

SolidWorks was chosen as it can easily handle our geometry containing constricted openings and sharp angles without the need to defeature the model.

SolidWorks Flow Simulation provides an exceptionally efficient automatic mesher for both fluid and solid regions and boundaries with mesh refinement appropriate to geometrical or physical requirements. In SolidWorks Flow Simulation the internal flow space containing the fluid is not modelled as a discrete domain in the design. This makes the 3D analysis of the geometry easy.

The first design chosen has a larger slit size with the intention of obtaining an increased mass flow rate at the expense of loss of outlet velocity(refer Fig.4(a)). On analysis it was observed that the first design does not provide sufficient thrust as the outlet velocity was too low. In order to overcome this drawback, a CD nozzle type arrangementFig.4(b) was added to the outflow section of the airfoil. This helped in increasing the exit velocity, but it did not produce sufficient thrust. The third design Fig.4(c) was created by decreasing the throat size to 3 mm and this design successfully provided the required thrust with uniform flow.

III. RESULTS AND DISCUSSION

3.1. Analysis Of Bladeless Thruster

The design conditions applied were based on the dimensions of the EDF available. A 64mm 4500 rpm EDF was chosen for the study based on the availability. Hence, the inlet duct diameter was fixed at a diameter of 64mm. The maximum hydraulic diameter of the thruster outlet was 200mm.

Since mass flow rate is required as an inlet boundary condition during CFD analysis, it was calculated using equation 1 and 2 as shown below

$$v=(\pi x N x D)/60$$
$$=(3.14x4500x0.064)/60.$$
$$= 15.08 \text{ m/s} \quad \text{.....(1)}$$
$$m= \rho x A x v$$
$$= 1.225 \text{ x } (3.14 \text{ x } (0.064\text{^}2)/4) \text{ x} 15.08$$
$$= 0.0594 \text{ kg/s} \quad \text{.....(2)}$$

Here, ‘v’ is velocity, ‘N’ is the rpm of the motor, ‘D’ denotes the diameter of the fan, ‘m’ represents the mass flow rate, ‘A’ is the area encompassed by the fan and ‘v’ in equation 2 is the velocity calculated from equation 1.

The drawbacks of design 1 were that the exit mass flow rate obtained was very small and negligible and outlet velocity obtained was much less than the inlet velocity. Hence,the thrust obtained was very small. The drawbacks of design 2, which was designed with the aim of increasing both the mass flow rate and the velocity at the outlet by employing a convergent-divergent passage at the exit of the airfoil, were that the mass flow rate obtained was nearly the same as that of the inlet but the velocity was much less than that obtained at the outlet of design.

The drawbacks of both design 1 and design 2 were overcome in design 3 with a throat size of 3mm Fig.4(c)and sufficient thrust was obtained. In order to further compare the designs obtained, a few parameters were considered, the results of which are described in the next section. The consolidated results of the 3D flow analysis of the three designs are as given in Table 1.

	DESIGN 1	DESIGN 2	DESIGN 3
Mass Flow Rate at inlet	0.06 kg/s	0.06 kg/s	0.06kg/s
Velocity at inlet	15.5 m/s	15.5 m/s	15.5m/s
Mass Flow Rate at outlet	0.00020 kg/s	0.061 kg/s	0.0676kg/s
Velocity at Outlet	5.2764 m/s	4.6177 m/s	27.175m/s
Thrust	0.9311 N	1.2148 N	2.7547N
Thruster Mass Flow Rate	0.1021 kg/s	0.0841 kg/s	0.29621kg/s
Thruster Velocity	1.9716 m/s	2.4458 m/s	5.85714m/s

Table 1: 3D flow analysis of the three designs

3.2. Simulations and Experimental Results

The first parameter considered was the Throat Sizewhich would control the two main contributing factors to thrust- velocity and mass flow rate. It was observed that with a smaller throat size, the mass flow rate was slightly more than the inlet mass flow rate. Also, the exit velocity at the outlet was high, thus giving a considerable amount of thrust. The Coanda effect takes place effectively with a smaller size.

The next parameter considered was theLength of the Inlet Duct. Two variants were tried in each of the design. The first version was with an inlet duct length was 30 mm, which means that the EDF was placed far away from the thruster ring. The second case was where the EDF was placed close to the thruster ring, where the duct length was 10mm. It was observed that placing the EDF closer to the ring helps generate a more uniformly distributed flow at the exit of the thruster. When the EDF was placed far from the ring, greater outflow was observed from the top of the ring and almost no flow was obtained from the bottom of the ring (the section near the inlet).

Another parameter analyzed was the Taper Angleof the ring cross-section. A taper angle of 15o and 20o was chosen for the study. It was seen that the taper angle does not contribute significantly to the final thrust obtained. Hence no taper angle was chosen for the final design in order to reduce constraints and restrictions on manufacturing.

The next parameter chosen for analysis was Hydraulic Diameter. It was observed that the best results were obtained for an optimum hydraulic diameter of 200mm. Increasing the hydraulic diameter to 300mm or 250mm produced a lower thrust, and decreasing the hydraulic diameter to

150mm gave a non-uniform flow at the exit. The increment in mass flow rate is quite small and negligible although the cross-sectional area increases as the hydraulic diameter increases. The details of the values obtained are as shown in Table 2.

Hydraulic Diameter	150mm	200mm	250mm	300mm
Mass Flow Rate at inlet	0.06 kg/s	0.06 kg/s	0.06 kg/s	0.06 kg/s
Velocity at inlet	26.39 m/s	15.224 m/s	15.2 m/s	15.467 m/s
Mass Flow Rate at outlet	0.058kg/s	0.059 kg/s	0.067 kg/s	0.066 kg/s
Velocity at Outlet	76.83 m/s	44.98 m/s	27.17 m/s	19.87 m/s
Thrust	6.04 N	3.61129 N	2.75477 N	2.248 N
Thruster Mass Flow Rate	0.285kg/s	0.306 kg/s	0.296 kg/s	0.267 kg/s
Thruster Velocity	16.00 m/s	9.55 m/s	5.875 m/s	3.796 m/s

Table 2: values obtained for various Hydraulic Diameter.

The velocity contours for the three different cross-sections are as shown in Fig.5(a),(b) and (c). It is observed that Design 2 gives a symmetric flow at the exit, but thrust produced is very low. Hence, Design 3 is considered to be the most apt design for our thruster.

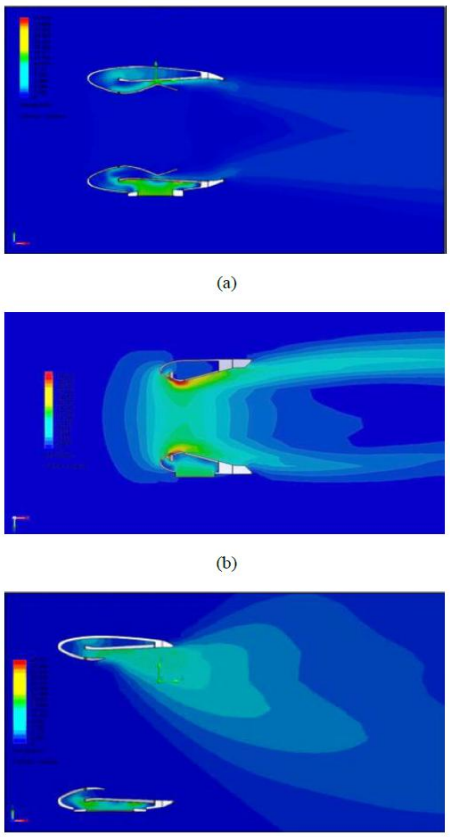

(a)

(b)

(c)

Fig.5. Velocity Cut-Plot of (a)Design 1 cross-section (b)Design 2 cross-section (c)Design 3 cross-section with 200mm Hydraulic Diameter.

The next parameter analyzed was the position of the inlet duct. In previously conducted analysis, the inlet duct was placed at the center of the ring thruster. Considering a forward position that is closer to the leading edge resulted in a lower thrust,but an aft position,i.e. near the trailing edge shows a slight increase in thrust.The results are as shown in Table 3.

Position of Inlet Duct	Aft (near Trailing Edge)	Middle	Forward (near Leading Edge)
Mass Flow Rate at inlet	0.06 kg/s	0.06 kg/s	0.06 kg/s
Velocity at inlet	14.7 m/s	15.47 m/s	15.27 m/s
Mass Flow Rate at outlet	0.066 kg/s	0.064 kg/s	0.067 kg/s
Velocity at Outlet	44.2 m/s	43.2 m/s	27.15 m/s
Thrust	3.825 N	3.725 N	2.75 N
Thruster Mass Flow Rate	0.24 kg/s	0.25 kg/s	0.29 kg/s
Thruster Velocity	7.55 m/s	7.73 m/s	5.77 m/s

Table 3: Values obtained for various position of the inlet duct.

3.3. Prototyping

3D printing was considered as the most apt method for validating our prototype. After some research, it was agreed that the fastest and the cheapest method would be 3D printing. The material used was PLA (Poly Lactic Acid). In order to minimize the use of support structures, which would have to be removed separately, the thruster ring was divided into smaller parts.

The prototype was used to validate the simulated results. The weight of the model was found to be 449g. The prototype used to validate results is as shown in Fig.6.

Fig.6. Thruster Prototype.

IV. CONCLUSION

The bladeless thruster designed was successfully analysed taking into consideration variations in parameters like Throat Size, Length of Inlet Duct, Taper Angle, Hydraulic Diameter and Position of Inlet Duct. Based on the 3D Flow analysis using SolidWorks, a bladeless thruster that provides sufficient thrust was achieved as shown in Fig.7.The manufacturing and design limitations have been identified through comparisons between computational and experimental data. Further probing must be carried out on the nature of flow and its influence on the mixing region.

The thrust produced may be further increased by increasing the inlet mass flow rate by using a higher powered EDF or a compressor. The bladeless thruster so devised may be used for a UAV Application which would be greatly beneficial in terms of safety.

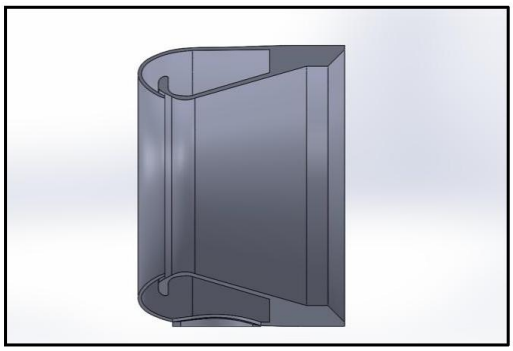

Fig.7. Section View of the Design 3 Thruster.

ACKNOWLEDGMENTS

The satisfaction on successful of this task would be incomplete without the mention of the people who made it possible. We would like to express our gratitude and respect to Dr CPS Prakash, Prinicipal, Dayananda Sagar College of Engineering for his constant support and encouragement. We would also like to thank Dr. Hareesha NG, Head of the Department, Aeronautical Engineering, Dayananda Sagar College of Engineering for his guidance, supervision and valuable suggestions for the successful completion of this project on time. We also take this opportunity to thank all the staff members of the Aeronautical Engineering Department who have rendered their wholehearted support for the timely completion of this project.

REFERENCE

[1] Daniel Valdenegro, Austin Capunay, Daniel Gonzalez,
[2] Luis Rodolfo Garcia Carrillo , Pablo Rangel 2018, Improving Safety: Design and Development of a Bladeless Thruster for Autonomous Multicopters, DOI: 10.1109/ICUAS.2018.8453474
[3] Hossein Afshin, Mohammad Jafari, Bijan Farhanieh, Atta Sojoudi, 2015, Numerical investigation of geometric parameter effects on the aerodynamic performance of aBladeless fan
[4] Edgar Herrera, retrieved from https://www.yankodesign.com/2017/08/18/the-dyson-of-drones/
[5] Ruixiong Li, Huanran Wang, Erren Yao, Meng Li and Weigang Nan, 2017, Experimental study on bladeless turbine using incompressible working medium, DOI: 10.1177/1687814016686935
[6] José Luis Córdova, HooshangHeshmat, 2017, A Bladeless Turbocompressor Concept: Shear Driven Gas Compression With Deformable Structures: Part 2 — Operating Principles and Theory, DOI: 10.1115/POWER-ICOPE2017-3375
[7] Lasse C . M¨ansson, Simon H. Traberg-Larsen, 2014, Flow Characteristics of the Dyson Air Multiplier
[8] M. Jafari, H. Afshin†, B. Farhanieh and H. Bozorgasareh, Numerical Aerodynamic Evaluation and Noise Investigation of a Bladeless Fan - Journal of Applied Fluid Mechanics, Vol. 8, No. 1, pp. 133-142, 2015.
[9] AlexandruDumitrache, Florin Frunzulica, Tudor Ionescu, Coanda Effect On The Flows Through Ejectors and Channels - Scienific Research and EducationintheAir Force, June 2018

★★★